Chalcogenide Letters Vol. 21, No. 3, March 2024, p. 275 - 284

The influence of substrate temperature on structural and optical characterization of nanostructured SnS thin films

A. A. Mansour[a], H. A. Salman[b], S. A. Abdul Wahab[c], N. F. Habubi[c], S. S. Chiad[d,*], Z. S. A. Mosa[c], Y. H. Kadhim[d]
[a]*Ministry of Education/ Directorate of Education Baghdad Governorate / Al-Karkh third, Baghdad, Iraq*
[b]*Department of Solar Energy Research, / Al- Nahrain Nanorenewable Energy Research Center, Al-Nahrain University, Baghdad, Iraq*
[C]*Department of Radiation and Sonar Technologies, Alnukhba University College, Baghdad, Iraq*
[d]*Department of Physics, College of Education, Mustansiriyah University, Baghdad, Iraq*
[e]*Department of Pharmacy, Al-Manara College for Medical Science, Iraq*
[f]*Department of Optics Techniques, Al-Mustaqbal University College, Babylon, Iraq*

To grow SnS films, the spray pyrolysis deposition (SPD) process is applied. The films were deposited at various substrate temperatures (ST) of 400, 450, and 500 degrees Celsius for two hours. Through XRD analysis, the impact of S_T on the structure was investigated. Peak (113) crystallite sizes were 13.16, 21.48, and 38.87 nm, respectively, at base temperatures of (400, 450, and 500) ^oC. The effect of ST on the structure was examined using XRD analysis. A predominat Peak at (113) plane. The crystallite sizes at base temperatures of (400, 450, and 500) ^oC were 13.16, 21.48, and 38.87 nm, respectively.

(Received December 1, 2023; Accepted March 19, 2024)

Keywords: SnS, Thin film, Spray pyrolysis, Physical properties, AFM

1. Introduction

In the 1970s and 1980s, SnS attracted attention because of its possible use as an optical storage medium. However, recent studies have examined its potential as a solar cell or photovoltaic system due to its inexpensive cost, high absorption coefficient, and low toxicity [1]. SnS is a p-type semiconductor with an optical bandgap that ranges from 1.2 to 1.5 eV [2–3]. Many applications, including photovoltaic devices [4-5], gas sensors [6-7], transistors [7], and intercalation battery systems [8], benefit from the convenience of this chemical. SnS can be deposited using a variety of methods, including spray pyrolysis [17], sol-gel [15], RF-magnetron sputtering [13], SILAR [9], PLD [10], electrodeposition [11], EBE [12], and CBD [14]. Spray pyrolysis deposition has created SnS nanostructures [18-20]. Spray pyrolysis deposition is a well-known, straightforward, and low-temperature deposition technique capable of being utilized over large areas with little effort [21]. The characterization of films by SPD can be controlled by several parameters, namely base temperature [22]. The present work deals with the S_T and their impact on the properties of the SnS films by SPD.

2. Experimental

SnS films were grown using the SPD method. Tin sulfide was prepared using a combination of 0.1 M of $SnCl_4.5H_2O$ and 0.1 M of SC $(NH_2)_2$ resolved in deionized water. This

* Corresponding author: dr.sami@uomustansiriyah.edu.iq
https://doi.org/10.15251/CL.2024.213.275

solution is produced at 400, 450, and 500 ^{o}C on a glass base. The base-to-spout distance of 28 cm, the spraying rate of 4 mL/min, the spraying period of 10, followed by a 1.5-minute break to prevent base cooling, and the transporter gas of N2 were determined to be the ideal values. The results obtained from the gravimetric approach are 300 ± 30 nm. With a double-beam spectrophotometer ((Shimatzu Japan)), the transmittance is measured. While AFM (AA3000 SPM) was used to get surface topography, XRD (SHIMADZU XRD-6000) was used to locate the film structure.

3. Results and discussion

Fig. 1 illustrates XRD spectra of deposited films. The film possesses multiple peaks allocated to the (113), (200), (105), (115), (212), and (106) planes, which give it its polycrystalline structure of orthorhombic SnS phases (according to ICDD card number (79-2193) [18]. Table 1 shows the crystallite sizes of the prepared film with base temperatures (T_a).

Sherrer's formula [23, 25] is used to calculate the average crystalline size (D):

$$D = \frac{K\lambda}{\beta cos\theta} \tag{1}$$

where λ = (0.154nm), k = 0.9, θ is Bragg's angle. Film grown with 400^{o}C has D equal to 13.166 nm of the peak (113). When increasing the base temperature from (450-500^{o}C) the crystallite size increases to (13.16-38.873nm), and microstrain value decreases from 0.0263 to 0.089 (Line^{-2}.m^{-1}). The increase in D values contributes to small crystallites merging to form larger crystallites. All the results agree with the references [19].

The lattice strain (ε) can be achieved by using the relation [26-28]:

$$\varepsilon = \frac{\beta cos\theta}{4} \tag{2}$$

(δ) can be obtained by using the relation [29-31]:

$$\delta = \frac{1}{D^2} \tag{3}$$

Figures 2 (a, b, c, and d) represent β , D, ε and the δ of SnS thin films at different S_T.

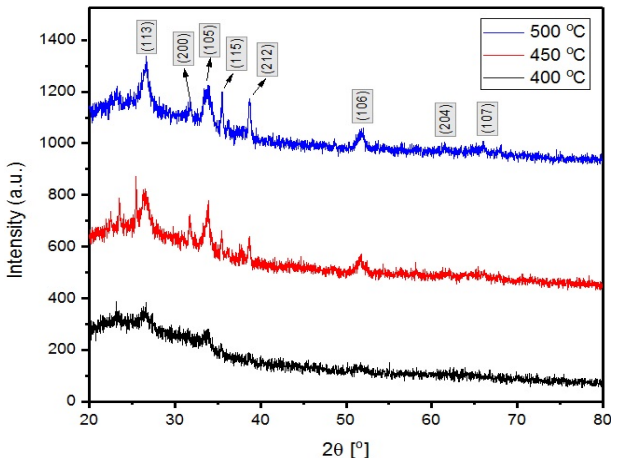

Fig. 1. XRD styles of grown films.

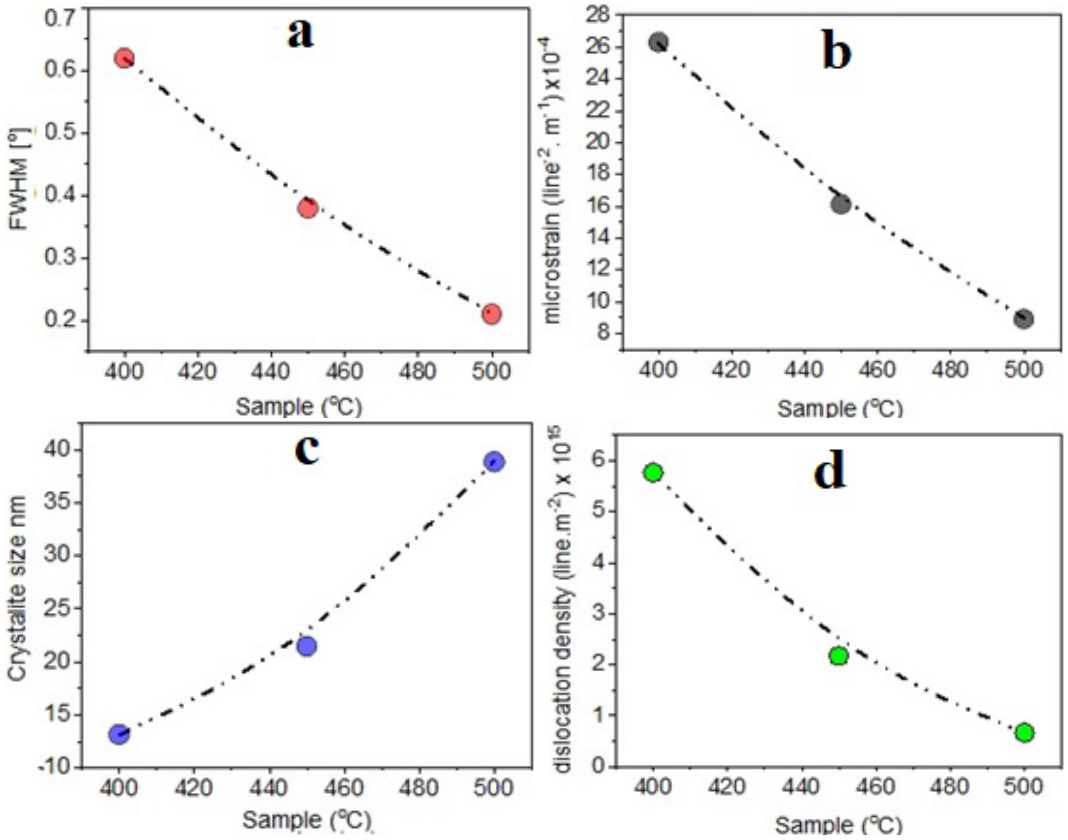

Fig. 2. (a) FWHM, (b) D, (c) ε, and (d) δ of intended films.

Table 1. Structural parameters of grown films.

Samples °C	(hkl) Plane	2Θ (°)	FWHM (°)	(D) (nm)	ε (Line^{-2}.m^{-1}) ×10^{-2}	(δ) (Line. m^{-2}) ×10^{15}	a (Å)	
							Standard	Calculated
400	(113)	26.64	0.62	13.166	26.32	5.77	4.162	4.164
450	(113)	26.64	0.38	21.482	16.15	2.17	4.162	4.160
500	(113)	26.64	0.21	38.873	8.97	6.61	4.162	4.160

AFM photographs with different base temperatures of 400, 450, and 500 °C are shown in Figures 3, 4, and 5. The films' average roughness (Ra) dropped from 4.39 nm to 1.57 nm when ST increased from 450 °C to 500 °C. The inactivation of the tin separation process on the surface could cause this. Films developed at 450 °C had Ra of 4.39 nm and an average diameter of 70 nm, while Ra at 400 °C (3.07 nm) had an average diameter Dav of 60 nm. In addition, the vacancy part over the surface decreased and S_T increased from 450 to 500 °C (Table 2). As a result, compared to films developed at 400 °C and 450 °C, the film roughness at 500 °C base was softer. When S_T increases, Table 2's Dav, RMS, and Ra values demonstrate the formation of a high number of smaller-sized crystallites. This effect might be explained by using ST to produce a larger density of nucleation centers [20].

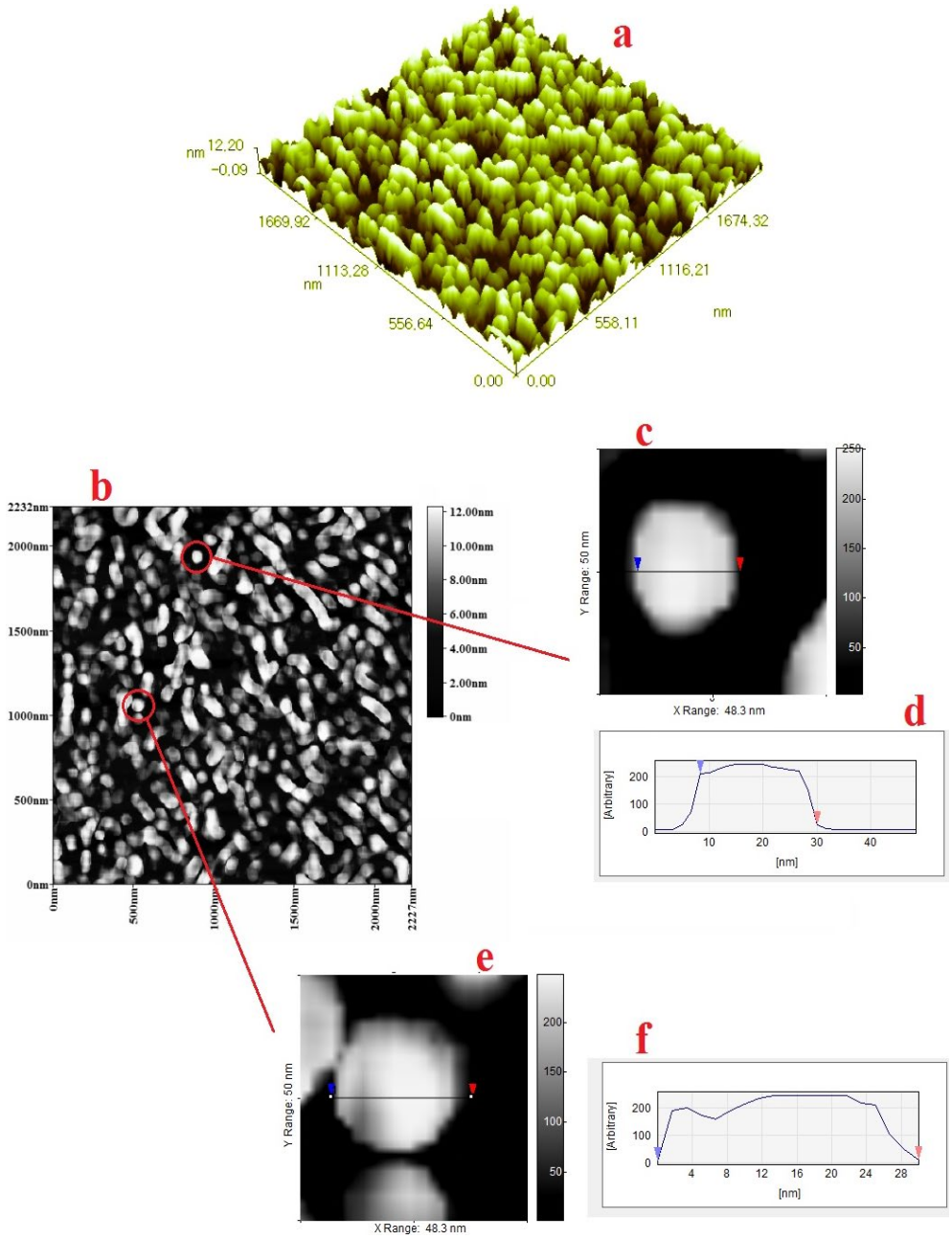

Fig. 3. AFM Images at base temperatures of 400 °C.

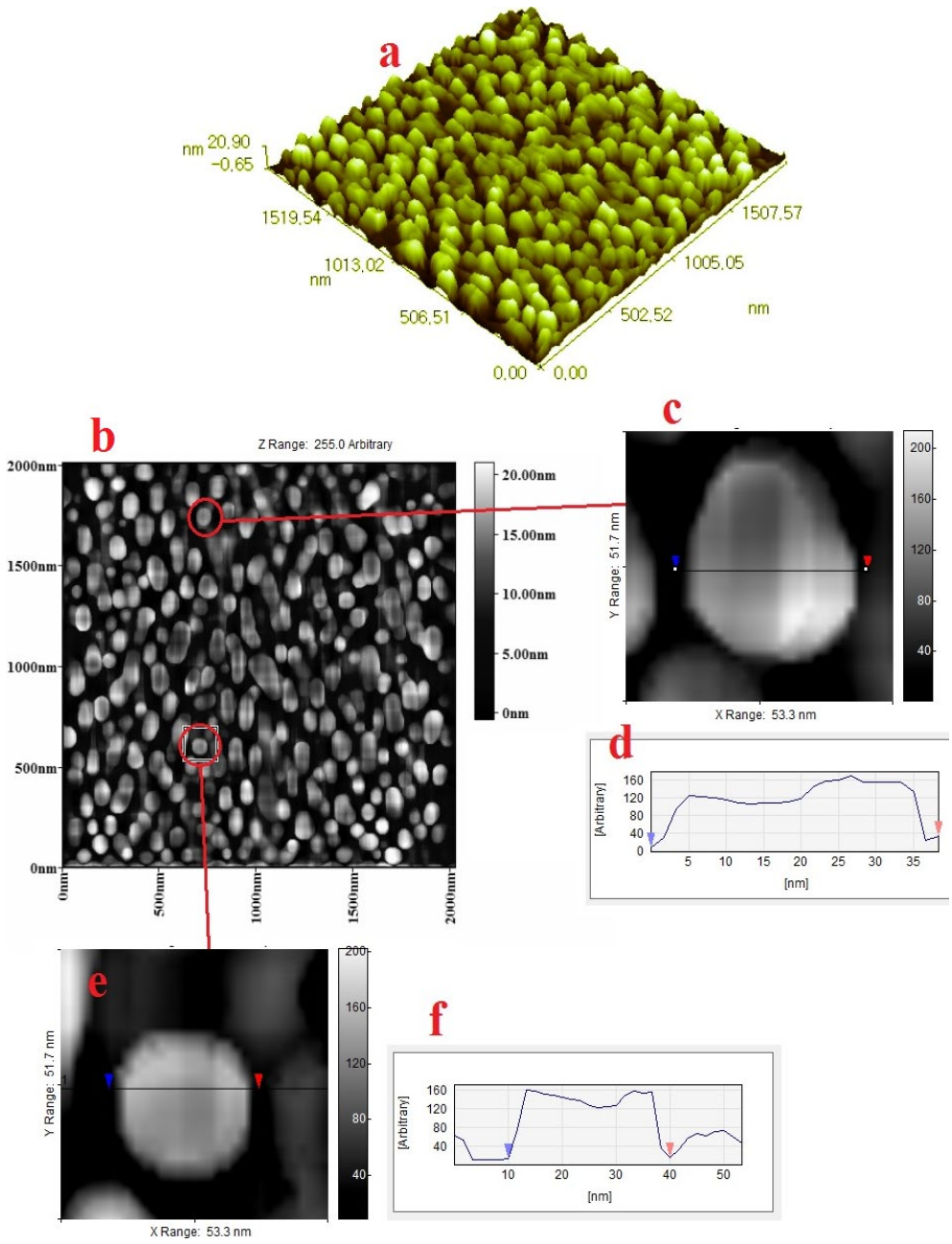

Fig. 4. AFM Images of S_T at 450 ^oC.

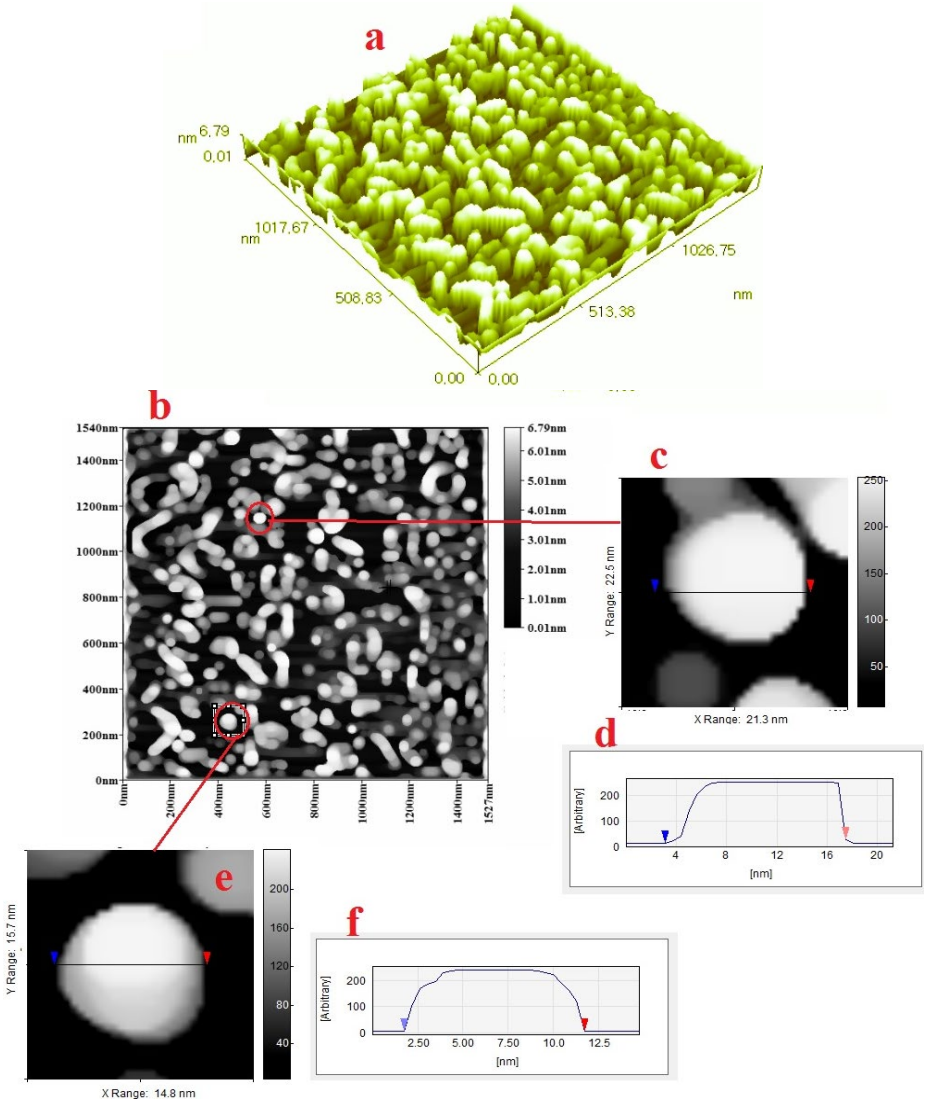

Fig. 5. AFM images of S_T at 500 ^oC.

Table 2. Surface morphology of SnS films at 400, 450 and 500 ^oC base temperatures.

Samples ^oC	**D_{av} nm**	**R_a nm**	**RMS nm**
400	60	3.07	3.55
450	70	4.39	5.14
500	80	1.57	3.1.83

Experimental measurements are usually made in terms of percentage transmittance (T), which is defined as [33-35]:

$$T\% = \frac{I}{I_o}\% \tag{4}$$

where I is the light intensity after it passes through the sample and Io is the initial light intensity. (T) spectra in UV-visible regions for (400, 450, and500˚C) have been illustrated in Fig. 6. T was increased via the increase in T_a. A maximum T of 80% was found at T_a of 400^{o}C [36-38]. The rise

in T is related to crystallinity enhancement when increased S_T. The energy bandgap E_g was located via equation 4 [39-41]:

$$(\alpha h\nu)^n = B(h\nu - E_g) \tag{4}$$

where B is constant, n = 2 for direct transition. Fig. 7. Shows that the optical bandgap increases with decreasing S_T from 3.23eV for the film annealed at 400°C. While at 450°C to 500°C, E_g decreased from 3.1 eV to 3.06 eV [42-44].

The absorption coefficient (α) of SnS is gained via equation 5 [44-46]:

$$\alpha = 2.303\, A/d \tag{5}$$

where d and A represent film thickness and absorbance, respectively. Figure (8) displays α versus wavelength. α is decreased with increasing of λ and S_T. Values of α are (>10^4 cm^{-1}) [47-49], suggesting the existence of direct transition. The results display that the absorption coefficient is increased from (2x10^4-3.75x$10^4$$cm^{-1}$) with an increase in S_T. This result agrees with reference [52, 53].

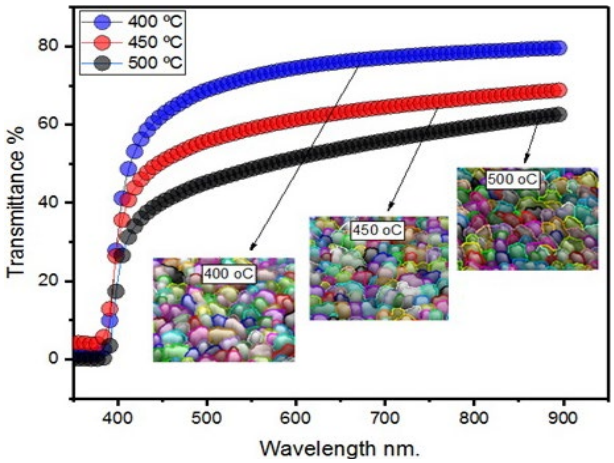

Fig. 6. Transmittance of SnS thin films at different S_T.

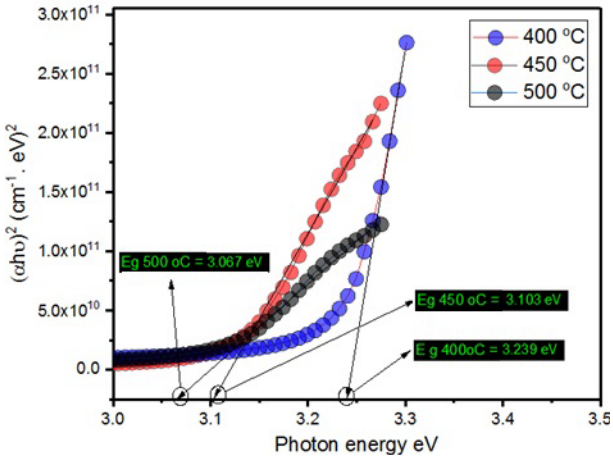

Fig. 7. Direct transition of the intended films.

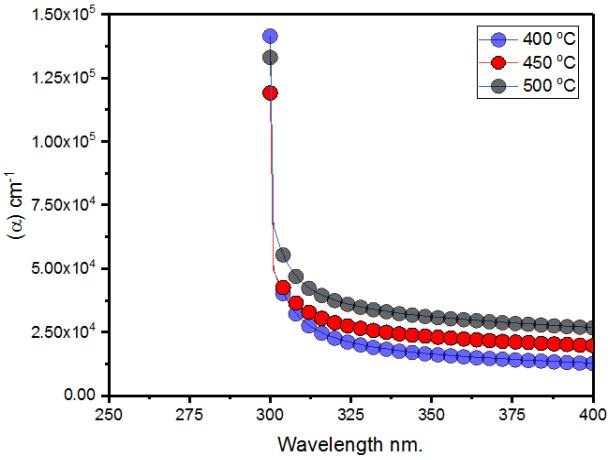

Fig. 8. α of the intended films.

4. Conclusion

Using CPD, SnS thin films were produced with good base adhesion at three different base temperatures (400, 450, and 500 ^{o}C). Film polycrystallinity is seen in XRD patterns, where the (113) direction has a strong peak. The size of the crystallites ranged from 13 to 38 nm, and the intensity peak of the films increased as the base temperature rose. The average particle size, as determined by AFM images, ranged from 60 to 80 nm as ST grew. At 500 ^{o}C ST, the absorption coefficient was 3.75X10^{4} cm^{-1}. As ST climbed, the optical bandgap fell and demonstrated a minimum of 3.06 eV for the 500 ^{o}C base. Ultimately, the findings indicated that S_T might enhance the SnS nanostructured films regarding crystallite size.

Acknowledgements

The authors commend Alnukhba University College and Mustansiriyah University for their assistance.

References

[1] M. C. Rao, M. S Shekhawat, International Journal of Modern Physics: Conference Series, 22, 576-582 (2013); http://doi.org/10.1142/s2010194513010696
[2] D. T. Read, A. A. Volinsky, In Physics, Mechanics, Design, Reliability, Packaging, A135–A180 (2007); http://doi.org/10.1007/0-387-32989-7_4
[3] M. Leach,, K. T. R. Reddy, M. V. Reddy, J. K. Tan, D. Y. Jang, R. W. Miles, In Energy Procedia (Vol. 15, pp. 371–378) (2012); https://doi.org/10.1016/j.egypro.2012.02.045
[4] V. V. Mohan, K .C. Akshaya, A. S. Asha, M. K. Jayaraj, K. P. Vijayakumar, Materials Today: Proceedings, 39, 1978-1980 (2021); http://doi.org/10.1016/j.matpr.2020.08.512
[5] L. Solymar, D. Walsh, & R. R. A. Syms, Semiconductors (Vol. 1). Oxford University Press(2018); https://doi.org/10.1093/oso/9780198829942.003.0008.
[6] D. Vikraman, S. Thiagarajan, K. Karuppasamy, A. Sanmugam, J.-H. Choi,, K. Prasanna, T. Maiyalagan, M. Thaiyan, H.-S. Kim, Applied Surface Science, 479, 167–176 (2019); https://doi.org/10.1016/j.apsusc.2019.02.056
[7] R. Higler, J.S prakel, Scientific Reports, 7(1), 12634 (2017); https://doi.org/10.1038/s41598-017-12730-8.
[8] O. O. Abegunde, E. T. Akinlabi, O. P. Oladijo, S. Akinlabi, A. U. Ude, AIMS Materials Science, 6(2), 174–199 (2019); https://doi.org/10.3934/matersci.2019.2.174

[9] M. A. M. Hassoon, Journal of Applied Physics, 101(9) (2015); http://doi.org/10.1063/1.2729450
[10] K. H. Jebur, N. J. Mohammed, Al-Mustansiriyah Journal of Science, 32(4), 60-66 (2021); http://doi.org/10.23851/mjs.v32i4.993
[11] S. A. Hasan, J. A. Salman, S. S. Al-Jubori, Al-Mustansiriyah Journal of Science, 32(4), 21-25 (2021); http://doi.org/10.23851/mjs.v32i4.1034
[12] A. A. Z. Alaabedin, B. H. Hamza, A. Mu. Abdual-Majeed, S. F. Bamsaoud, Al-Mustansiriyah Journal of Science, 34 (3), 115-123 (2023); https://doi.org/10.23851/mjs.v34i3.1339
[13] T., Tanaka, T. Nagatomo, D. Kawasaki, M. Nishio, Q. Guo, A. Wakahara, H. Ogawa, Journal of Physics and Chemistry of Solids, 66(11), 1978-1981 (2005); http://doi.org/10.1016/j.jpcs.2005.09.037
[14] S. Kumar, Spectrochimica Acta Part A Molecular and Biomolecular Spectroscopy 115 C, 840-844 (2013); https://doi.org/10.1016/j.saa.2013.06.112
[15] S. Baco, A. Chik, F. M. d. Yassin, J. Sci. Technol., 4, 61–72(2012); http://penerbit.uthm.edu.my/ojs/index.php/JST/article/view/468.
[16] W. Wang, H. Shen, H. Yao, J. Li, J. Jiao, Journal of Materials Science: Materials in Electronics, 26(3), 1449-1454 (2015); http://doi.org/10.1007/s10854-014-2560-4
[17] T. Sall, B. M. Soucase, M. Mollar, J. A. Sans, Journal of Electronic Materials, 46(3), 1714-1719 (2017); http://doi.org/10.1007/s11664-016-5215-9.
[18] G. G. Ninan, C. S. Kartha, K. P. Vijayakumar, Solar Energy Materials and Solar Cells, 157, 229-233 (2016); http://doi.org/10.1016/j.solmat.2016.05.059
[19] M. Devika, N. K. Reddy, K. Ramesh, H. R. Sumana, K. R. Gunasekhar, E. S. R. Gopal, K. R. ReddySemiconductor science and technology, 21(10), 1495–1501 (2016); http://doi.org/10.1088/0268-1242/21/10/024
[20] R. Kaur, S. B. Narang, S. K. Tripathi, Journal of Materials Science: Materials in Electronics, 32(4), 4883-4890 (2021); https://doi.org/10.1016/j.matpr.2021.09.330
[21] G. G. Ninan, C. S. Kartha, K. P. Vijayakumar Solar Energy Materials and Solar Cells, 157, 229-233 (2016); http://doi.org/10.1016/j.solmat.2016.05.059
[22] V. V. Mohan, K. C. Akshaya, A. S. Asha,, M. K. Jayaraj, K. P. Vijayakumar, Materials Today: Proceedings, 39, 1978-1980 (2021); http://doi.org/10.1016/j.matpr.2020.08.512
[23] R. S Ali, N. A. H. Al Aaraji, E. H. Hadi, N. F. Habubi, S. S. Chiad, Journal of Nanostructuresthis link is disabled, 10(4), 810–816 (2020); https://doi: 10.22052/jns.2020.04.014
[24] A. A. Khadayeir, R. I. Jasim, S. H. Jumaah, N. F, Habubi, S. S. Chiad, Journal of Physics: Conference Series,1664 (1) (2020); https://doi.org/10.1088/1742-6596/1664/1/012009
[25] S. S Chiad,, A. S. Alkelaby, K. S. Sharba,, Journal of Global Pharma Technology, 11 (7), 662-665, (2020); https://doi.org/10.1021/acscatal.1c01666
[26] Chiad, S.S., Noor, H.A., Abdulmunem, O.M., Habubi, N.F., Journal of Physics: Conference Series 1362(1), 012115 (2019); https://doi.org/10.1088/1742-6596/1362/1/012115
[27] R. S. Ali, M. K. Mohammed, A. A. Khadayeir, Z. M. Abood, N. F. Habubi and S. S. Chiad, Journal of Physics: Conference Series, 1664 (1), 012016 (2020); https://doi:10.1088/1742-6596/1664/1/012016
[28] A. S. Al Rawas, M. Y. Slewa, B. A. Bader, N. F. Habubi, S. S. Chiad, Journal of Green Engineering,10 (9), 7141-7153 (2020); https://doi.org/10.1021/acsami.1c00304
[29] K. Y. Qader, R. . Ghazi, A. M. Jabbar, K. H. Abass, S. S. Chiad, Journal of Green Engineering, 10 (10), 7387-7398, 2020. https://doi.org/10.1016/j.jece.2020.104011
[30] S. S. Chiad, N. F. Habubi, W. H. Abass, M.H. Abdul-Allah, Journal of Optoelectronics and Advanced Materials, 18(9-10), 822-826, (2016).
[31] A. Ghazai, K. Qader, N. F. Hbubi, S. S. Chiad, O. Abdulmunem, IOP Conference Series: Materials Science and Engineering, 870 (1), 012027 (2020); https://doi.org/ 10.1088/1757-899X/870/1/012027
[32] R. Kihal, H. Rahal, A. M. Affoune, M. Ghers, Journal of Electrochemical Science and Technology, 8(3), 206–214 (2017); https://doi.org/10.33961/JECST.2017.8.3.206.

[33] N. N. Jandow, M. S. Othman, N. F.Habubi, S. S. Chiad, K. A. Mishjil, I. A. Al-Baidhany, Materials Research Express, 6 (11), (2020); https://doi.org/10.1088/2053-1591/ab4af8
[34] E. S. Hassan, K. Y. Qader, E. H. Hadi, S. S. Chiad, N. F. Habubi, K. H. Abass, Nano Biomedicine and Engineering, 12(3), pp. 205-213 (2020); https://doi.org/10.5101/nbe.v12i3.p205-213
[35] M. D. Sakhil, Z. M. Shaban, K. S. Sharba, N. F. Habub, K. H. Abass, S. S. Chiad, A. S. Alkelaby, NeuroQuantology, 18 (5), 56-61 (2020); https://doi.org/10.14704/nq.2020.18.5.NQ20168
[36] N. Y. Ahmed, B. A. Bader, M. Y. Slewa, N. F. Habubi, S. S. Chiad, NeuroQuantology, 18(6), 55-60 (2020); https://doi.org/10.1016/j.jlumin.2021.118221
[37] Khadayeir, A. A., Hassan, E. S., Mubarak, T. H., Chiad, S.S., Habubi, N. F., Dawood, M.O., Al-Baidhany, I. A., Journal of Physics: Conference Series, 1294 (2) 022009(2019); https://doi.1088/1742-6596/1294/2/022009
[38] A. J. Ghazai, O. M. Abdulmunem, K. Y. Qader, S. S. Chiad, N. F. Habubi, AIP Conference Proceedings 2213 (1), 020101 (2020); https://doi.org/10.1063/5.0000158
[39] H. A. Hussin, R. S. Al-Hasnawy, R. I. Jasim, N. F. Habubi, S. S. Chiad, Journal of Green Engineering, 10(9), 7018-7028 (2020); https://doi.org/10.1088/1742-6596/1999/1/012063
[40] S. S. Chiad, H. A. Noor, O. M. Abdulmunem, N. F. Habubi, M. Jadan, J. S. Addasi, Journal of Ovonic Research, 16 (1), 35-40 (2020). https://doi.org/10.15251/JOR.2020.161.35
[41] H. T. Salloom, E. H. Hadi, N. F. Habubi, S. S. Chiad, M. Jadan, J. S. Addasi, Digest Journal of Nanomaterials and Biostructures, 15 (4), 189-1195 (2020); https://doi.org/10.15251/DJNB.2020.154.1189
[41] S. S. Chiad, T. H. Mubarak, International Journal of Nanoelectronics and Materials, 13 (2), 221-232 (2020).
[42] O. M. Abdulmunem, A. M. Jabbar, S. K. Muhammad, M. O. Dawood, S. S. Chiad, N. F. Habubi, Journal of Physics: Conference Series,1660 (1), 012055 (2020); https://doi.org/ 10.1088/1742-6596/1660/1/012055
[43] E. H. Hadi, M. A. Abbsa, A. A. Khadayeir, Z. M. Abood, N. F. Habubi, and S.S. Chiad, Journal of Physics: Conference Series, 1664 (1), 012069 (2020); https://doi.org/ 10.1088/1742-6596/1664/1/012069
[44] M. S. Othman, K. A. Mishjil, H. G. Rashid, S. S. Chiad, N. F. Habubi, I. A. Al-Baidhany, Journal of Materials Science: Materials in Electronics, 31(11), 9037-9043 (2020); https://doi.org/10.1007/s10854-020-03437-0
[45] E. H. Hadi, D. A. Sabur, S. S. Chiad, N. F. Habubi, K., Abass, Journal of Green Engineering, 10 (10), 8390-8400 (2020); https://doi.org/10.1063/5.0095169
[46] Hassan, E.S., Mubarak, T.H., Chiad, S.S., Habubi, N.F., Khadayeir, A.A., Dawood, M.O., Al-Baidhany, I. A. , Journal of Physics: Conference Series, 1294(2), 022008 (2019); https://doi.1088/1742-6596/1294/2/022008
[47] M.O. Dawood, S.S. Chiad, A.J. Ghazai, N.F. Habubi, O.M. Abdulmunem, AIP Conference Proceedings 2213, 020102,(2020); https://doi.org/10.1063/5.0000136
[48] A. A. Khadayeir, E. S. Hassan, S. S. Chiad, N. F. Habubi, K. H. Abass, M. H. Rahid, T. H. Mubarak, M. O. Dawod, and I.A. Al-Baidhany, Journal of Physics: Conference Series 1234 (1), 012014, (2019); https://doi.1088/1742-6596/1234/1/012014
[49] N. Y. Ahmed, B. A. Bader, M. Y. Slewa, N. F. Habubi, S. S. Chiad, NeuroQuantology, 18(6), 55-60 (2020); https://doi.org/10.14704/nq.2020.18.6.NQ20183
[50] N. N. Jandow, N. F. Habubi, S. S. chiad, I. A. Al-Baidhany and M. A. Qaeed, International Journal of Nanoelectronics and Materials, 12 (1), 1-10 2019.
[51] R. S. Ali, H. S. Rasheed, N. F. Habubi, S.S. Chiad, Chalcogenide Letters, , 20 (1), 63–72 (2023; https://doi.org/10.15251/CL.2023.201.63
[52] B. A. Bader, S. K. Muhammad, A. M. Jabbar, K. H. Abass, S. S. Chiad, N. F. Habubi, J. Nanostruct, 10(4): 744-750, (2020); https://doi.org/ 10.22052/JNS.2020.04.007
[53] K. H. Jebur, N. J. Mohammed, Al-Mustansiriyah Journal of Science, 32(4), 60-66 (2021); http://doi.org/10.23851/mjs.v32i4.993